

# Explore the Potential Performance of Vision-and-Language Navigation Model: a Snapshot Ensemble Method

Wenda Qin<sup>1</sup>, Teruhisa Misu<sup>2</sup>, Derry Wijaya<sup>1</sup>

<sup>1</sup>Boston University

111 Cummington Mall, Boston MA 02215

wdqin, wijaya@bu.edu

<sup>2</sup>Honda Research Institute USA, Inc.

70 Rio Robles, San Jose, CA 95134

tmsu@honda-ri.com

## Abstract

Vision-and-Language Navigation (VLN) is a challenging task in the field of artificial intelligence. Although massive progress has been made in this task over the past few years attributed to breakthroughs in deep vision and language models, it remains tough to build VLN models that can generalize as well as humans. In this paper, we provide a new perspective to improve VLN models. Based on our discovery that snapshots of the same VLN model behave significantly differently even when their success rates are relatively the same, we propose a snapshot-based ensemble solution that leverages predictions among multiple snapshots. Constructed on the snapshots of the existing state-of-the-art (SOTA) model  $\odot$ BERT and our past-action-aware modification, our proposed ensemble achieves the new SOTA performance in the R2R dataset challenge in Navigation Error (NE) and Success weighted by Path Length (SPL).

## 1 Introduction

Given instruction in texts and visual inputs describing the surrounding environment, a Vision-and-Language Navigation (VLN) agent controls an agent to complete a set of goals listed in the instruction. Building a good VLN system is difficult due to the fact that it needs to understand vision and language information and coordinate them well.

Recent advancements in computer vision and natural language processing and the advent of better vision-language models (Sundermeyer, Schlüter, and Ney 2012; Vaswani et al. 2017; Lu et al. 2019; Tan and Bansal 2019) along with the effort to prepare large scale realistic datasets (Chang et al. 2017) has enabled rapid development of VLN systems. Among all current VLN datasets, the R2R dataset (Anderson et al. 2018) is a dataset based on real photos taken in indoor environments. It attracts massive attention for its simple-form task, which at the same time requires complex understanding in both images and texts.

To obtain better performance in R2R, various studies in the past have discussed how to adjust the best vision/language models at the time for the R2R VLN task (Anderson et al. 2018; Majumdar et al. 2020; Hong et al. 2021).

Previous studies have also made efforts to prevent overfitting due to the limited size of the R2R dataset (Fried et al. 2018; Liu et al. 2021; Li et al. 2019; Hao et al. 2020).

In this paper, we offer a new perspective for analyzing the R2R VLN model that focuses on the by-products of the model training process: snapshots. Snapshots are the saved parameters of a model at various intervals during training. Although all snapshots have the same goal as the model, their parameters are different due to the ongoing optimization. We discover that some of the best snapshots at various intervals saved during training shared similar navigation success rates while making significantly diverse errors. Based on such observation, we construct our VLN system with an ensemble of snapshots instead of just one. Through experiments, we found out that such an ensemble can take advantage of its members and thus significantly improve the navigation performance.

In addition, to allow more model variants in the ensemble, we also propose a novel modification of an existing state-of-the-art (SOTA) model for VLN i.e., the VLN $\odot$ BERT (Hong et al. 2021). Our ensemble, which consists of snapshots of both models: the VLN $\odot$ BERT model and our proposed modification: the past-action-aware VLN $\odot$ BERT model—achieves a new SOTA performance in the single-run setting of the R2R dataset.

To conclude, our contributions are as follows:

- We discover that the best snapshots of the same model behave differently while having similar navigation success rates. Based on this observation, we propose a snapshot ensemble method to take advantage of the different snapshots.
- We also propose a past-action-aware modification on the current best VLN model: the VLN $\odot$ BERT. It creates additional variant snapshots to the original model with equivalent navigation performance.
- By combining the snapshots from both the original and the modified model, our ensemble achieves a new SOTA performance on the R2R challenge leaderboard in the single-run setting.<sup>1</sup>

<sup>1</sup>Our method is noted as “SE-Mixed (Single-Run)” in

- We evaluate the snapshot ensemble method on two different datasets and apply it with two other VLN models. The evaluation results show that the snapshot ensemble also improves performance on more complicated VLN tasks and with different model architectures.

## 2 Related Works

### 2.1 Vision-and-language Navigation datasets

Teaching a robot to complete instructions is a long-existing goal in the AI community (Winograd 1971). Compared to GPS-based navigation, VLN accepts surrounding environments as visual inputs and correlates them with instruction in human language. Most VLN datasets in the past are based on synthesized 3-D scenes (Kolve et al. 2017; Brodeur et al. 2017; Wu et al. 2018; Yan et al. 2018; Song et al. 2017). Recently, the emergence of data based on real-life scenarios allows VLN systems to be developed and tested in realistic environments. Specifically, 3-D views from Google Street View<sup>2</sup> and Matterport3D datasets (Chang et al. 2017) allow people to build simulators that generate navigation data from photos taken in real life. Different from the previous datasets, the R2R dataset that we use consists of navigations in real indoor environments. Concretely, the R2R dataset provides  $\sim 15,000$  instructions and  $\sim 5,000$  navigation paths in 90 indoor scenes. Since its construction, people have proposed variants of the R2R dataset to address certain shortcomings of the original one (Ku et al. 2020; Jain et al. 2019; Hong et al. 2020b; Krantz et al. 2020). However, the community still considers the R2R dataset a necessary test for evaluating all kinds of VLN systems for indoor navigation.

### 2.2 VLN systems for navigation in R2R dataset

To improve navigation performance in the R2R dataset, various models and techniques have been proposed. Fried et al. (2018) and Tan, Yu, and Bansal (2019) further developed the LSTM (Sundermeyer, Schlüter, and Ney 2012) + soft-attention (Luong, Pham, and Manning 2015) baseline system (Anderson et al. 2018). Majumdar et al. (2020) proposed a VLN system based on ViBERT (Lu et al. 2019) to replace the LSTM + soft-attention architecture for better image and text understanding. Recently, Chen et al. (2021); Wang et al. (2021); Hong et al. (2020a) proposed VLN systems based on graph models. In terms of techniques, Fried et al. (2018) built a speaker model for data augmentation. Ma et al. (2019b,a) introduced regularization loss and backtracking; Tan, Yu, and Bansal (2019) improved the dropout mechanic in its VLN model; Li et al. (2019); Hao et al. (2020) improved the models’ initial states by pre-training it on large-scale datasets; and Hong et al. (2021) developed a recurrent VLN model (VLN $\odot$ BERT) based on BERT structure for single-run setting in VLN. Liu et al. (2021) provides further data augmentation by splitting and mixing scenes.

Previous work that shared the closest idea to us is Hu et al. (2019), which proposed a mixture of VLN models. However,

the leaderboard webpage: <https://eval.ai/web/challenges/challenge-page/97/leaderboard>

<sup>2</sup><https://www.google.com/streetview/>

each of their models is trained with different inputs. In this paper, we build an ensemble based on snapshots of the *same* model.

### 2.3 Ensemble

The concept of applying ensemble in neural network models appeared very early in the machine learning community (Hansen and Salamon 1990). There are well-known ensemble techniques such as Bagging (Breiman 1996), Random forests (Ho 1995), and boosting (AdaBoost) (Freund and Schapire 1997). However, applying such ensembles to deep learning models directly is very time-consuming. There are previous works that provide ensemble-like solutions for deep learning models Xie, Xu, and Chuang (2013); Moghimi et al. (2016); Laine and Aila (2016); French, Mackiewicz, and Fisher (2017). Our work is inspired by the idea of “snapshot ensemble” from Huang et al. (2017), which constructs the ensemble from a set of snapshots collected in local minima. Different from the previous work, we collect snapshots based on training intervals and success rates. Also, we apply beam search to optimize the combination of snapshots to be in the ensemble.

## 3 Preliminaries

### 3.1 Vision-and-language Navigation in R2R dataset

Navigation in R2R consists of three parts: instruction  $I$ , scene  $S$ , and path  $P$ . The instruction  $I$  is a sequence of  $L$  words in the vocabulary  $W$ :  $I = \{w_1, w_2, \dots, w_L \mid w_i \in W, 1 \leq i \leq L\}$ . The scene  $S$  is a connected graph that contains viewpoints  $V$  and the edges  $E$  that connect viewpoints:  $S = \{V, E\}$ . For viewpoint  $v_i \in V$  where the agent stands, there’s a panoramic view  $O_i$  to describe the visual surroundings of the agent. To be more precise,  $O_i$  is a set of 36 views  $O_i = \{o_{i,j}\}_{j=1}^{36}$  that a camera captured in the viewpoint from different horizontal and vertical directions. A viewpoint  $v_a$  is connected (“navigable”) to another viewpoint  $v_b$  when you could directly walk from  $v_a$  to  $v_b$  in the real environment that  $S$  represents. The path  $P$  is a sequence of viewpoints, which starts from the starting viewpoint, and ends in the destination viewpoint:  $P = \{v_1, v_2, \dots, v_n \mid v \in V\}$ .  $v_1$  is the initial position of the agent.

A VLN model for the R2R navigation task works as a policy function with the instruction  $I$  and the panoramic view  $O_i$  of a certain viewpoint as inputs:  $\pi_\theta(I, O_i)$ . At each time step  $t$ , the policy function predicts an action  $a_t \sim \pi_\theta(I, O_i)$ , and tries to get as close as possible to the ground truth destination  $v_n$  in  $P$  at the end.

After the agent chooses to stop or the number of its actions exceeds a limit, its last viewpoint  $v_{end}$  will be evaluated. If  $v_{end}$  is within 3 meters of  $v_n$  from ground-truth path  $P$ , the navigation is considered to be successful or failed otherwise.

There are three different settings for the VLN task in R2R: single-run, pre-explore, and beam search. In this paper, we focus on the single-run setting. The “single-run” setting requires the agent to finish the navigation with minimum actions taken and without prior knowledge of the environment.

### 3.2 VLN $\odot$ BERT model

We apply our modification and snapshot ensemble on the VLN $\odot$ BERT model proposed by Hong et al. (2021).<sup>3</sup> The model currently holds the best performance for the single-run setting in the R2R dataset (Liu et al. 2021). In this section, we will have a brief recap of this model. A simplified visualization of the model structure is in Figure 1.

Before computing the prediction of actions, the model selects a set of candidate views from  $O_i$ . After that, the VLN $\odot$ BERT model projects the candidate views and the instruction into the same feature space. We discuss this process in detail in Appendix A. Eventually, we have a vector of instruction features  $F_{instruction}^{t=1} = [f_{cls}, f_{w_1}, \dots, f_{w_L}, f_{sep}]$  and a vector of candidate action features  $F_{candidate}^t = [f_{a_1}, \dots, f_{a_n}, f_{a_{stop}}]$  as inputs of the action prediction.

At the first time step,  $F_{instruction}^{t=1}$  is sent to a 9-layer self-attended module. The word features are thus attended to the  $f_{cls}^{t=1}$  feature. The model then appends  $f_{cls}^{t=1}$  to  $F_{candidate}^{t=1}$  from  $F_{instruction}^{t=1}$ . After that, a cross-attention sub-module attends the remaining elements in  $F_{instruction}^{t=1}$  to both  $F_{candidate}^{t=1}$  and  $f_{cls}^{t=1}$ . Lastly, another sub-module computes the self-attention of the instruction-attended  $[F_{candidate}^{t=1}, f_{cls}^{t=1}]$ . Such cross and self sub-modules build up the cross + self-attention module in figure 1. The process repeats for four layers and the attention scores between  $f_{cls}^{t=1}$  and each elements in  $F_{candidate}^{t=1}$  of the last layer are the prediction scores of each action  $p_1, \dots, p_n, p_{stop}$ . Additionally, the  $f_{cls}^t$  in the output is sent to a cross-modal matching module. The output of the module is used as  $f_{cls}^{t+1}$  in the next time step while other features in  $F_{instruction}^{t=1}$  remains unchanged. The cross and self attention computation will be repeated to compute action predictions for the rest of time steps.

The VLN $\odot$ BERT model minimizes two losses: imitation learning loss and reinforcement learning loss:

$$\mathcal{L}_{\text{original}} = -\lambda \sum_{t=1}^T a_t \log(p_t) - \sum_{t=1}^T a_s \log(p_t) A(t)$$

where  $a_t$  is the teacher action (one-hot encoded action that gets closest to the destination),  $p_t$  is the probability of the taken action,  $a_s$  is the action taken and  $A(t)$  is the advantage value at time step  $t$ , computed by the A2C algorithm (Mnih et al. 2016).  $\lambda = 0.5$  is a hyper-parameter that balances the weights of imitation learning loss and reinforcement learning loss.

## 4 Proposed Method

### 4.1 Differences of Snapshots in the Same VLN model

Like other machine learning models, VLN $\odot$ BERT chooses the best snapshot by validation to represent the trained

<sup>3</sup>(Hong et al. 2021) proposed two VLN $\odot$ BERT models in their work. The VLN $\odot$ BERT model we used here is the LXMERT-based VLN $\odot$ BERT model pre-trained by PREVALENT (Hao et al. 2020). For the other one, which is BERT-based and pre-trained by OSCAR (Li et al. 2020), we call it OSCAR-init VLN $\odot$ BERT to distinguish it from the PREVALENT-initialized one.

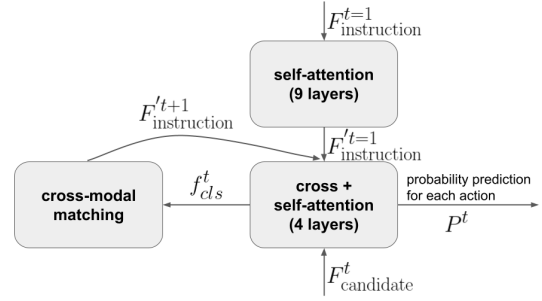


Figure 1: A visualization of the VLN $\odot$ BERT model. The instruction feature first passes through a self-attention module and then attends to a candidate feature vector through a cross-self-attention module. The candidate feature then self-attended itself in the same module. After four layers of computation, the last layer outputs the probabilities of each action and sends the  $cls$  feature to a cross-modal matching module. The output will replace the  $cls$  features in the instruction vector for the next time step.

model. We train the VLN $\odot$ BERT model and observe its validation success rates, as measured on the val\_unseen split of R2R, of the snapshots saved in the training process. As shown in Appendix B Figure 1, we saw that the success rate fluctuates drastically over time. This fluctuation is however not seen in the training loss. As shown in Appendix B, figures 2 and 3, both imitation and reinforcement learning losses drop consistently with time. This interesting discovery leads us to further investigate whether the snapshots that perform similarly (in terms of success rates) might behave differently with respect to the errors that they make.

We set up an experiment designed as follows: we train the VLN $\odot$ BERT model for 300,000 iterations and save the best snapshot in the validation split for every 30,000 iterations. The top-5 snapshots among them are shown in Table 1. We chose the best two snapshots, namely the snapshots with 62.32% and 61.60% success rates. We then count the navigations that only one of the snapshots failed, both of the snapshots failed or none of the snapshots failed. Our result shows that 563 navigations ended with different results between the best and the second-best snapshots, approximately 24% of the validation data. In comparison, the difference in their success rate is only 0.72%. The massive difference between 24% and 0.72% suggests that the agents of the two snapshots have different navigation behaviors even though they are almost equal in success rates. Naturally, we wonder if we could leverage both of their behaviors and thus create a better agent. One of the techniques we find to be effective for this problem is the snapshot ensemble that we discuss in the next section.

### 4.2 Snapshot Ensemble for VLN $\odot$ BERT models

A snapshot is a set of saved parameters of a model during a particular time in training. Naturally, the first thing to do to set up the ensemble is to decide what snapshots to save during training. According to Huang et al. (2017), the en-

Snapshot Period	Success Rate in val.unseen Split
90K - 120K	62.32%
240K - 270K	61.60%
210K - 240K	61.56%
60K - 90K	61.52%
180K - 210K	61.30%

Table 1: The navigation success rates for the top-5 snapshots of VLN $\odot$ BERT in 10 periods of a 300,000-iteration training cycle.

semble mechanic does the best when “the individual models have low test error and do not overlap in the set of examples they misclassify”. Therefore, we want to save snapshots that are “different enough” while doing well individually. Our approach is as follows (where snapshots and ensembles are evaluated on the validation set):

- For a training cycle of  $N$  iterations, we evenly divide it into  $M = \{m_1, m_2, \dots, m_M\}$  periods (assuming  $N$  is divisible by  $M$ ).
- For each period  $m_i$ , we save the snapshot  $s_i$  with the highest success rate in the validation split.
- The saved snapshots will be the candidates to build the ensemble:  $\{s_1, \dots, s_M\}$ .

Among the candidates snapshot saved this way, we conduct a beam search with size  $l = 3$  to construct the ensemble of maximum size  $k$ . The process is as follows:

- Evaluate all possible ensembles of size 1, that is:  $\{\{s_1\}, \{s_2\}, \dots, \{s_M\}\}$
- Keep the top- $l$  ensembles in the previous step. For each kept ensemble, evaluate all possible ensembles of size 2 that contain the kept snapshot(s). E.g., say  $\{s_2\}$  is one of the top- $l$  ensembles of size 1, the ensembles of size 2 to be evaluated related to  $\{s_2\}$  are:  $\{\{s_2, s_1\}, \{s_2, s_3\}, \dots, \{s_2, s_M\}\}$ .
- Keep the top- $l$  ensembles of size 2 from the previous step. Then we repeat the process for size-3 ensembles, so on and so forth. The evaluation stops when we finish evaluating the ensembles of size  $k$ .
- In the end, we choose the ensemble with the highest success rate among all the ensembles evaluated during the whole process.

The approximate number of evaluations needed for our beam search strategy is  $O(Mlk)$  when  $M \gg k$ , which is much smaller than the cost of an exhaustive search  $O(\min(M^k, M^{(M-k)}))$ .

During the evaluation, the ensemble completes a navigation task as follows: at each time step, the instruction inputs and the visual inputs of the current viewpoint are sent to each snapshot in the ensemble. Each snapshot then gives its predictions on the available actions. After that, the agent sums those predictions up and takes the corresponding action. At the end of the time step, each snapshot uses the action taken to update its own states. We visualize the ensemble navigation workflow in Figure 2. We do not apply normalization on the prediction scores of snapshots to allow model confidence as the score weights.

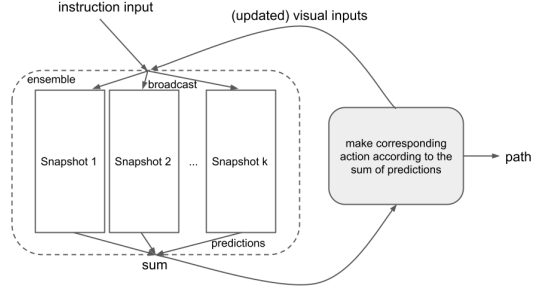


Figure 2: The workflow of the snapshot ensemble in the recurrent navigation process. The inputs broadcast to all snapshots, and the ensemble sums their predictions to make action at every time step.

### 4.3 A past-action-aware VLN $\odot$ BERT model

We saw a significant improvement in the snapshot ensemble of the original VLN $\odot$ BERT model, as shown in Table 2. Still, we could improve the performance of the ensemble by adding more variant snapshots. To do that, we modify the VLN $\odot$ BERT model and combine the snapshots of the original and the modified model.

Our modification is based on the two ideas to improve the model: adding  $f_{cls}^t$  in the past time steps and regularizing the attention scores between  $f_{cls}^t$  and words in  $I$  based on the observation of OSCAR-init VLN $\odot$ BERT model in (Hong et al. 2021). The modification is visualized by the blue parts in figure 3.

At the beginning of each time step  $t > 1$ , we add a copy of the cross-modal matching output  $f_{cls}^{t-1}$  from the last time step to a  $F_{cls\_history}$  vector. At time step  $t$ ,  $F_{cls\_history} = [f_{cls}^{t-1}, \dots, f_{cls}^{t-1}]$ , re-indexed from 2 to  $t$ . We then concatenate  $F_{cls\_history}$  and  $[F_{candidate}^t, f_{cls}^t]$  as a large vector, and pass them through the cross + self-attention module. Note that we do not update the features in  $F_{cls\_history}$  during the attention computation. As a result, we will not only have the attention scores from the current  $f_{cls}^t$  to each word features in  $F_{instruction}^{t=1}$ , but also that from the  $F_{cls\_history}$  to  $F_{instruction}^{t=1}$  in the last layer outputs.

For each set of attention scores  $X_i = [x_1, \dots, x_L]$  from  $f_{cls}^i$  to each word in the instruction  $w_1, \dots, w_L$  where  $i \in [1, t]$ , we compute an “attention regularization” loss defined as follows:

$$\mathcal{L}_{\text{attention}_t} = \frac{1}{t} \sum_{i=1}^t \text{MSE}(\tanh(X_i), G_i)$$

“MSE” stands for Mean-Squared-Error and  $G_i = [g_{i,1}, \dots, g_{i,L}]$  is the “ground truth” values for the normalized attention scores  $\tanh(X_i)$ .  $G_i$  is computed based on the sub-instruction annotation from the Fine-Grained R2R dataset (FGR2R). Concretely, the FGR2R dataset divides the instructions in the R2R dataset into a set of ordered sub-instructions:  $I = [I_{sub_1}, I_{sub_2}, \dots, I_{sub_n}]$  where  $n$  is the number of sub-instructions the original instruction consists of. Each sub-instruction corresponds to one or a sequence of

viewpoints in the ground truth path  $P = \{v_1, v_2, \dots, v_m\}$ . To compute  $G_i$ , we first build a map from each viewpoint  $v_i$  in  $P$  to a specific sub-instruction in  $I$ . The map function is very straightforward: we choose the first sub-instruction  $I_{sub_i}$  in  $I$  that corresponds to  $v_i$  as the mapped sub-instruction. By doing so, each viewpoint  $v$  in  $P$  now has their own related sub-instruction  $I_{sub_i}$  in  $I$ . We then compute  $G_i = [g_1, \dots, g_L]$ , by the following step:

- find the viewpoint  $v_i$  where the agent stands at time step  $i$ . If  $v_i \notin P$ , we choose the viewpoint in  $P$  that is closest to  $v_i$  as the new  $v_i \in P$ .
- Since every  $v_i$  has its mapped  $I_{sub_i}$ , we compute each  $g_j \in G_i$  by:

$$g_j = \begin{cases} 1 & \text{if } w_j \in I_{sub_i}, \\ 0.5 & \text{if } w_j \in I_{sub_{i+1}}, \\ -1 & \text{otherwise.} \end{cases}$$

We compute each  $\mathcal{L}_{\text{attention}_t}$  and the total loss becomes:

$$\mathcal{L}_{\text{past-action-aware}} = \mathcal{L}_{\text{original}} + \alpha \sum_{t=1}^T \mathcal{L}_{\text{attention}_t}$$

$\alpha = 0.5$  is a hyper-parameter and  $T$  is the total time steps.

The added *cls* history vector provides additional information to the model during action prediction. In addition, the attention regularization forces the VLN $\odot$ BERT model to align attention scores to words that correspond to the agent’s actions without performance (success rate) drop. The visualization of how the attention score changes as the agent moves in its path are given in appendix C.

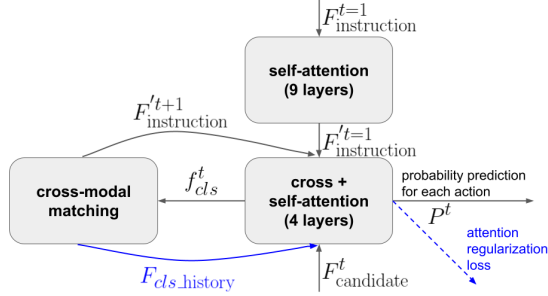


Figure 3: The structure of past-action-aware VLN $\odot$ BERT model. The blue parts are the modification added to the original structure. A *cls* history vector is added to keep track of the past  $f^t_{cls}$ . An attention regularization loss is added to regularize the attention scores between  $f^t_{cls}$  at each time step and relevant words in the instruction (visualization is given in appendix C).

## 5 Experiment

We run the following experiments to evaluate the performances of snapshot ensembles in different models and datasets:

- We evaluate the performance of snapshot ensemble on the R2R dataset, including the ensemble built from the original model snapshots and the ensemble built from both the original and the modified model snapshots.

- We also apply snapshot ensemble on the OSCAR-init VLN $\odot$ BERT model from Hong et al. (2021) and the Env-Drop model from Tan, Yu, and Bansal (2019). We evaluate and compare their ensemble performances on the R2R dataset against their best single snapshot.
- We evaluate the performance of snapshot ensemble on the R4R dataset, which is a larger VLN dataset than R2R and with more complicated navigation paths.

### 5.1 Dataset Setting and Evaluation Metrics

We use the R2R train split as training data, val\_unseen split as validation data, and test split to evaluate the ensemble. For the R4R dataset, we also use the train split as the training data. As there’s no test split in the R4R dataset, we divide the val\_unseen split into two halves. The two halves do not share scenes in common. We construct the snapshot ensemble on one half and evaluate it on the other half.

We adopt four metrics for evaluation: Success Rate (SR), Trajectory Length (TL), NavigationError (NE), and Success weighted by Path Length (SPL). SR is the ratio of successful navigation numbers to the number of all navigations (higher is better). TL is the average length of the model’s navigation path (lower is better). NE is the average distance between the last viewpoint in the predicted path and the ground truth destination viewpoint (lower is better); SPL is the path-length weighted success rate compared to SR (higher is better).

### 5.2 Training Setting and Hard/Software Setup

We train the VLN $\odot$ BERT and the OSCAR-init VLN $\odot$ BERT model with the default 300,000 iterations. We run an ablation study to decide  $M = 10, k = 4$  for constructing the ensemble (the candidate number for beam search is  $2M$  when mixing the original and modified models. In R4R, we set  $k = 3$  to shorten the evaluation time). Appendix D describes the ablation study result. For other parameters, we use the default given by the authors.<sup>4</sup>

We set the pseudo-random seed to 0 for the training process. We run the training code under Ubuntu 20.04.1 LTS operating system, GeForce RTX 3090 Graphics Card with 24GB memory. It takes around 10,000 MB of graphics card memory to evaluate an ensemble of 4 snapshots with batch size 8 inputs. The code is developed in Pytorch 1.7.1, and CUDA 11.2. The training takes approximately 30 - 40 hours to finish. The beam search evaluation is done in 3 - 5 hours.

## 6 Results

### 6.1 Evaluation Results of our proposed methods on R2R dataset

We evaluate our modification of the VLN $\odot$ BERT model, the snapshot ensembles of original-only and mixed (original and modified) snapshots on the R2R test split. Table 2 shows the evaluation results of our model and ensembles. The past-action-aware modified model has a similar

<sup>4</sup>We do not adopt the cyclic learning rate schedule (Loshchilov and Hutter 2016) suggested in Huang et al. (2017) that forces the model to generate local minima. Our trial experiment result shows there’s no significant improvement by doing so in this task.

Model	R2R val_unseen				R2R test			
	TL↓	NE↓	SR↑	SPL↑	TL↓	NE↓	SR↑	SPL↑
Random	9.77	9.23	16	-	9.89	9.79	13	12
Human	-	-	-	-	11.85	1.61	86	76
Seq2Seq-SF (Anderson et al. 2018)	8.39	7.81	22	-	8.13	7.85	20	18
Speaker-Follower (Fried et al. 2018)	-	6.62	35	-	14.82	6.62	35	28
PRESS (Li et al. 2019)	10.36	5.28	49	45	10.77	5.49	49	45
EnvDrop (Tan, Yu, and Bansal 2019)	10.7	5.22	52	48	11.66	5.23	51	47
AuxRN (Zhu et al. 2020)	-	5.28	55	50	-	5.15	55	51
PREVALENT (Hao et al. 2020)	10.19	4.71	58	53	10.51	5.3	54	51
RelGraph (Hong et al. 2020a)	9.99	4.73	57	53	10.29	4.75	55	52
VLN $\odot$ BERT (Hong et al. 2021)	12.01	3.93	63	57	12.35	4.09	63	57
VLN $\odot$ BERT + REM (Liu et al. 2021)	12.44	3.89	63.6	57.9	13.11	3.87	<b>65.2</b>	59.1
Past-action-aware VLN $\odot$ BERT (ours)	13.2	3.88	63.47	56.27	13.86	4.11	62.49	56.11
VLN $\odot$ BERT Original Snapshot Ensemble (ours)	11.79	3.75	65.55	59.2	12.41	4	64.22	58.96
VLN $\odot$ BERT Past-action-aware Snapshot Ensemble (ours)	12.35	3.72	65.26	58.65	13.19	3.93	64.65	58.78
VLN $\odot$ BERT Mixed Snapshot Ensemble (ours)	12.05	<b>3.63</b>	<b>66.67</b>	<b>60.16</b>	12.71	<b>3.82</b>	65.11	<b>59.61</b>

Table 2: The evaluation results for our snapshot ensemble and past-action-aware VLN $\odot$ BERT models (bold is best). Our mixed snapshot ensemble achieved the new SOTA performance in NE and SPL, and only 0.09% worse than (Liu et al. 2021), which uses further data augmentation, in SR.

Model	R4R val_unseen_half				R4R val_unseen_full			
	TL↓	NE↓	SR↑	SPL↑	TL↓	NE↓	SR↑	SPL↑
Speaker-Follower	-	-	-	-	19.9	8.47	23.8	12.2
EnvDrop	-	-	-	-	-	9.18	34.7	21
VLN $\odot$ BERT + REM (Liu et al. 2021)	-	-	-	-	-	<b>6.21</b>	<b>46</b>	<b>38.1</b>
VLN $\odot$ BERT	13.76	7.05	37.29	27.38	13.92	6.55	43.11	32.13
VLN $\odot$ BERT Original Snapshot Ensemble (ours)	15.09	<b>7.03</b>	<b>39</b>	<b>28.66</b>	14.71	6.44	44.55	33.45

Table 3: Evaluation results on R4R dataset (bold is best). We also present the evaluation result of the full split with our constructed ensemble. The model gains  $> 1\%$  improvement from the original VLN $\odot$ BERT model after applying snapshot ensemble. Note that (Liu et al. 2021) uses further data augmentation, which is orthogonal to our approach. At the time of writing they have yet to release their code or dataset which might improve our performance further.

performance to the original model. Both snapshot ensembles significantly improve the performance of the model in NE, SR, and SPL. Specifically, the mixed snapshot ensemble achieved the new SOTA in NE and SPL while only 0.09% worse than VLN $\odot$ BERT + REM (Liu et al. 2021), which uses further data augmentation, in SR. At the time of writing, they have yet to release their code or dataset which may improve our results further.

Additionally, we evaluate whether the snapshot ensemble also improves different VLN models. We train an OSCAR-init VLN $\odot$ BERT (Hong et al. 2021), which is a BERT-structure model, and an EnvDropout model (Tan, Yu, and Bansal 2019) which has an LSTM plus soft-attention structure with their default training settings. We apply the snapshot ensemble on both and compare the ensemble’s performance with their best single snapshot on the R2R test split. Table 4 shows the evaluation result. Both ensembles consistently gained a more than 2% increase in SR and SPL compared to the best snapshot of the model. That suggests the snapshot ensemble is also able to improve the performances of other VLN models as well.

## 6.2 Evaluation Results of Snapshot Ensemble on R4R dataset

In addition to the R2R dataset, we evaluate the snapshot ensemble method on a more challenging dataset R4R (Jain et al. 2019). R4R dataset contains more navigation data and more complicated paths in more variant lengths. Table 3 shows the evaluation result between the best snapshot and the snapshot ensemble. We saw a more than 1% of increase in SR and SPL after applying snapshot ensemble. We also evaluate the same snapshot ensemble with all val\_unseen split data in R4R, as shown in Table 3.

## 7 Discussion

In this section, we discuss potential reasons why the snapshot ensemble works well in the VLN task. Additionally, we provide a case study in appendix E that qualitatively analyzes our proposed snapshot ensemble.

### 7.1 Ensemble is More Similar to Its Snapshots

To find out if the snapshot ensemble leverages the predictions of its snapshots, we analyze the errors that it makes in comparison to those of its snapshots (similar to our analysis in section 4.1), counting the distinctive failures of the snapshots and the ensemble on the validation set. We choose an ensemble of 3 snapshots with SR 65.43% obtained via

Model	R2R val_unseen				R2R Test			
	TL↓	NE↓	SR↑	SPL↑	TL↓	NE↓	SR↑	SPL↑
EnvDrop	<b>10.7</b>	5.22	52	48	<b>11.66</b>	5.23	51	47
EnvDrop Snapshot Ensemble	11.74	<b>4.9</b>	<b>53.34</b>	<b>49.49</b>	11.9	<b>4.98</b>	<b>53.58</b>	<b>50.01</b>
OSCAR-init VLN $\odot$ BERT	<b>11.86</b>	4.29	59	53	12.34	4.59	57	53
OSCAR-init VLN $\odot$ BERT Snapshot Ensemble	11.22	<b>4.21</b>	<b>59.73</b>	<b>54.76</b>	<b>11.74</b>	<b>4.36</b>	<b>59.72</b>	<b>55.35</b>

Table 4: The evaluation result of snapshot ensembles of EnvDrop and OSCAR-init VLN $\odot$ BERT for R2R val\_unseen split. Both models are consistently improved by the snapshot ensemble methods.

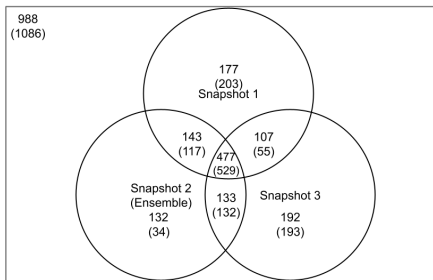


Figure 4: The Venn diagram on val\_unseen that counts the number of navigation that are failed by one or more snapshots. The numbers not in any circle are navigations that are succeeded by all 3 snapshots. The numbers in parenthesis are the counts when snapshot 2 is replaced by the ensemble.

beam search to visualize the shared failure cases among the three snapshots and the failure cases shared between snapshots 1, 3, and the ensemble (replacing snapshot 2). We draw the corresponding Venn diagram with and without the replacement, as shown in Figure 4. In comparison to snapshot 2, the ensemble shares more navigations that are succeeded/failed between itself and the two snapshots ( $529+1086 > 477+988$ ). Meanwhile, the number of navigations that are only failed by the ensemble is less than that of snapshot 2 ( $34 < 132$ ). These changes suggest that the ensemble behaves more similarly to its snapshot members than the replaced snapshot. We repeat this process by replacing snapshots 1 and 3 and obtain a similar result.

To understand the benefits of the ensemble acting more similarly to its snapshots, we count the successful navigations of the ensemble/snapshots in each scene. Table 5 shows the result. We find that each snapshot is good at different scenes. The ensemble either outperforms its snapshots or is comparable to the best snapshot in most scenes suggesting that the ensemble leverages the advantages of snapshots in different scenes to achieve better performance.

## 7.2 Ensemble Avoids Long Navigations

In our setting, the system forces the agent to stop when its taken actions are over 15. We call navigations that take the agent 15 or more actions to complete as Long Navigations (LNs). As ground truth navigation only needs 5 - 7 actions, we wonder if LN is harmful to the model performance. In table 6, we count the LNs for snapshots and the ensemble discussed in section 7.1 and compute the success rates when their navigation is an LN. We discovered that 5.5% to 10.5% of agent’s navigations are LNs. Meanwhile, LN has a high

likelihood ( $> 90\%$ ) of failing. As the ensemble has a much fewer number of LNs than its snapshots (131), we consider avoiding more LNs as one of the reasons why the ensemble outperforms single snapshots.

Scene	Ensemble	Snapshot 1	Snapshot 2	Snapshot 3
1	178	165	169	159
2	32	33	32	29
3	140	131	131	144
4	208	189	199	185
5	10	11	8	9
6	169	161	170	152
7	203	198	200	196
8	217	205	204	212
9	93	80	89	84
10	102	95	89	89
11	185	177	173	181

Table 5: The count of successful navigations for the ensemble and its snapshots in each scene on val\_unseen split.

	SR	LN Count	LN that fails (%)
Snapshot 1	61.52	172	159 (92.44%)
Snapshot 2	62.32	155	141 (90.97%)
Snapshot 3	61.3	246	223 (90.65%)
Ensemble	65.43	131	123 (93.89%)

Table 6: Long navigation (LN) for the ensemble and snapshots. The ensemble has fewer long navigation (131) when compared to its snapshot members.

## 8 Conclusion

In this paper, we discover differences in snapshots of the same VLN model. We apply the snapshot ensemble method that leverages the behaviors of multiple snapshots. By combining snapshots of the VLN $\odot$ BERT model and its past-action-aware modification that we propose, we achieve a new SOTA performance on the R2R dataset. We also show that our snapshot ensemble method works with different models and on more complicated VLN tasks. In the future, we will train the model with augmented data from Liu et al. (2021) and see if it improves performance. We will also apply our approach to pre-explore and beam search settings to see if ensemble methods can improve performance on these settings.

## References

Anderson, P.; Wu, Q.; Teney, D.; Bruce, J.; Johnson, M.; Sünderhauf, N.; Reid, I.; Gould, S.; and Van Den Hengel, A. 2018. Vision-and-language Navigation: Interpreting

- Visually-grounded Navigation Instructions in Real Environments. In *Proceedings of the IEEE Conference on Computer Vision and Pattern Recognition*, 3674–3683.
- Breiman, L. 1996. Bagging Predictors. *Machine learning* 24(2): 123–140.
- Brodeur, S.; Perez, E.; Anand, A.; Golemo, F.; Celotti, L.; Strub, F.; Rouat, J.; Larochelle, H.; and Courville, A. 2017. Home: A Household Multimodal Environment. *arXiv preprint arXiv:1711.11017*.
- Chang, A.; Dai, A.; Funkhouser, T.; Halber, M.; Niessner, M.; Savva, M.; Song, S.; Zeng, A.; and Zhang, Y. 2017. Matterport3D: Learning from RGB-D Data in Indoor Environments. *International Conference on 3D Vision (3DV)*.
- Chen, K.; Chen, J. K.; Chuang, J.; Vázquez, M.; and Savarese, S. 2021. Topological Planning with Transformers for Vision-and-Language Navigation. In *Proceedings of the IEEE/CVF Conference on Computer Vision and Pattern Recognition*, 11276–11286.
- French, G.; Mackiewicz, M.; and Fisher, M. 2017. Self-ensembling for Visual Domain Adaptation. *arXiv preprint arXiv:1706.05208*.
- Freund, Y.; and Schapire, R. E. 1997. A Decision-theoretic Generalization of On-line Learning and an Application to Boosting. *Journal of computer and system sciences* 55(1): 119–139.
- Fried, D.; Hu, R.; Cirik, V.; Rohrbach, A.; Andreas, J.; Morency, L.-P.; Berg-Kirkpatrick, T.; Saenko, K.; Klein, D.; and Darrell, T. 2018. Speaker-follower Models for Vision-and-language Navigation. *arXiv preprint arXiv:1806.02724*.
- Hansen, L. K.; and Salamon, P. 1990. Neural Network Ensembles. *IEEE transactions on pattern analysis and machine intelligence* 12(10): 993–1001.
- Hao, W.; Li, C.; Li, X.; Carin, L.; and Gao, J. 2020. Towards Learning a Generic Agent for Vision-and-language Navigation via Pre-training. In *Proceedings of the IEEE/CVF Conference on Computer Vision and Pattern Recognition*, 13137–13146.
- Ho, T. K. 1995. Random Decision Forests. In *Proceedings of 3rd international conference on document analysis and recognition*, volume 1, 278–282. IEEE.
- Hong, Y.; Rodriguez-Opazo, C.; Qi, Y.; Wu, Q.; and Gould, S. 2020a. Language and Visual Entity Relationship Graph for Agent Navigation. *arXiv preprint arXiv:2010.09304*.
- Hong, Y.; Rodriguez-Opazo, C.; Wu, Q.; and Gould, S. 2020b. Sub-instruction Aware Vision-and-language Navigation. *arXiv preprint arXiv:2004.02707*.
- Hong, Y.; Wu, Q.; Qi, Y.; Rodriguez-Opazo, C.; and Gould, S. 2021. VLN BERT: A Recurrent Vision-and-Language BERT for Navigation. In *Proceedings of the IEEE/CVF Conference on Computer Vision and Pattern Recognition*, 1643–1653.
- Hu, R.; Fried, D.; Rohrbach, A.; Klein, D.; Darrell, T.; and Saenko, K. 2019. Are You Looking? Grounding to Multiple Modalities in Vision-and-language Navigation. *arXiv preprint arXiv:1906.00347*.
- Huang, G.; Li, Y.; Pleiss, G.; Liu, Z.; Hopcroft, J. E.; and Weinberger, K. Q. 2017. Snapshot Ensembles: Train 1, Get M for Free. *arXiv preprint arXiv:1704.00109*.
- Jain, V.; Magalhaes, G.; Ku, A.; Vaswani, A.; Ie, E.; and Baldrige, J. 2019. Stay on the Path: Instruction Fidelity in Vision-and-language Navigation. *arXiv preprint arXiv:1905.12255*.
- Kolve, E.; Mottaghi, R.; Han, W.; VanderBilt, E.; Weihs, L.; Herrasti, A.; Gordon, D.; Zhu, Y.; Gupta, A.; and Farhadi, A. 2017. Ai2-thor: An Interactive 3D Environment for Visual AI. *arXiv preprint arXiv:1712.05474*.
- Krantz, J.; Wijmans, E.; Majumdar, A.; Batra, D.; and Lee, S. 2020. Beyond the Nav-graph: Vision-and-language Navigation in Continuous Environments. In *European Conference on Computer Vision*, 104–120. Springer.
- Ku, A.; Anderson, P.; Patel, R.; Ie, E.; and Baldrige, J. 2020. Room-across-room: Multilingual Vision-and-language Navigation with Dense Spatiotemporal Grounding. *arXiv preprint arXiv:2010.07954*.
- Laine, S.; and Aila, T. 2016. Temporal Ensembling for Semi-supervised Learning. *arXiv preprint arXiv:1610.02242*.
- Li, X.; Li, C.; Xia, Q.; Bisk, Y.; Celikyilmaz, A.; Gao, J.; Smith, N.; and Choi, Y. 2019. Robust Navigation with Language Pretraining and Stochastic Sampling. *arXiv preprint arXiv:1909.02244*.
- Li, X.; Yin, X.; Li, C.; Zhang, P.; Hu, X.; Zhang, L.; Wang, L.; Hu, H.; Dong, L.; Wei, F.; et al. 2020. Oscar: Object-semantics aligned pre-training for vision-language tasks. In *European Conference on Computer Vision*, 121–137. Springer.
- Liu, C.; Zhu, F.; Chang, X.; Liang, X.; and Shen, Y.-D. 2021. Vision-Language Navigation with Random Environmental Mixup. *arXiv preprint arXiv:2106.07876*.
- Loshchilov, I.; and Hutter, F. 2016. Sgdr: Stochastic Gradient Descent with Warm Restarts. *arXiv preprint arXiv:1608.03983*.
- Lu, J.; Batra, D.; Parikh, D.; and Lee, S. 2019. VILBERT: Pretraining Task-agnostic Visiolinguistic Representations for Vision-and-language Tasks. *arXiv preprint arXiv:1908.02265*.
- Luong, M.-T.; Pham, H.; and Manning, C. D. 2015. Effective Approaches to Attention-based Neural Machine Translation. *arXiv preprint arXiv:1508.04025*.
- Ma, C.-Y.; Lu, J.; Wu, Z.; AlRegib, G.; Kira, Z.; Socher, R.; and Xiong, C. 2019a. Self-monitoring Navigation Agent via Auxiliary Progress Estimation. *arXiv preprint arXiv:1901.03035*.
- Ma, C.-Y.; Wu, Z.; AlRegib, G.; Xiong, C.; and Kira, Z. 2019b. The Regretful Agent: Heuristic-aided Navigation Through Progress Estimation. In *Proceedings of the*

*IEEE/CVF Conference on Computer Vision and Pattern Recognition*, 6732–6740.

Majumdar, A.; Shrivastava, A.; Lee, S.; Anderson, P.; Parikh, D.; and Batra, D. 2020. Improving Vision-and-language Navigation with Image-text Pairs from the Web. In *European Conference on Computer Vision*, 259–274. Springer.

Mnih, V.; Badia, A. P.; Mirza, M.; Graves, A.; Lillicrap, T.; Harley, T.; Silver, D.; and Kavukcuoglu, K. 2016. Asynchronous Methods for Deep Reinforcement Learning. In *International conference on machine learning*, 1928–1937. PMLR.

Moghim, M.; Belongie, S. J.; Saberian, M. J.; Yang, J.; Vasconcelos, N.; and Li, L.-J. 2016. Boosted Convolutional Neural Networks. In *BMVC*, volume 5, 6.

Song, S.; Yu, F.; Zeng, A.; Chang, A. X.; Savva, M.; and Funkhouser, T. 2017. Semantic Scene Completion From a Single Depth Image. In *Proceedings of the IEEE Conference on Computer Vision and Pattern Recognition (CVPR)*.

Sundermeyer, M.; Schlüter, R.; and Ney, H. 2012. LSTM Neural Networks for Language Modeling. In *Thirteenth annual conference of the international speech communication association*.

Tan, H.; and Bansal, M. 2019. LXMERT: Learning Cross-modality Encoder Representations from Transformers. *arXiv preprint arXiv:1908.07490*.

Tan, H.; Yu, L.; and Bansal, M. 2019. Learning to Navigate Unseen Environments: Back Translation with Environmental Dropout. *arXiv preprint arXiv:1904.04195*.

Vaswani, A.; Shazeer, N.; Parmar, N.; Uszkoreit, J.; Jones, L.; Gomez, A. N.; Kaiser, Ł.; and Polosukhin, I. 2017. Attention is All You Need. In *Advances in neural information processing systems*, 5998–6008.

Wang, H.; Wang, W.; Liang, W.; Xiong, C.; and Shen, J. 2021. Structured Scene Memory for Vision-Language Navigation. In *Proceedings of the IEEE/CVF Conference on Computer Vision and Pattern Recognition (CVPR)*, 8455–8464.

Winograd, T. 1971. Procedures as a Representation for Data in a Computer Program for Understanding Natural Language. Technical report, MASSACHUSETTS INST OF TECH CAMBRIDGE PROJECT MAC.

Wu, Y.; Wu, Y.; Gkioxari, G.; and Tian, Y. 2018. Building Generalizable Agents with a Realistic and Rich 3D Environment. *arXiv preprint arXiv:1801.02209*.

Xie, J.; Xu, B.; and Chuang, Z. 2013. Horizontal and Vertical Ensemble with Deep Representation for Classification. *arXiv preprint arXiv:1306.2759*.

Yan, C.; Misra, D.; Bennet, A.; Walsman, A.; Bisk, Y.; and Artzi, Y. 2018. Chalet: Cornell House Agent Learning Environment. *arXiv preprint arXiv:1801.07357*.

Zhu, F.; Zhu, Y.; Chang, X.; and Liang, X. 2020. Vision-Language Navigation With Self-Supervised Auxiliary Reasoning Tasks. In *Proceedings of the IEEE/CVF Conference on Computer Vision and Pattern Recognition (CVPR)*.

# Supplementary Materials for “Explore the Potential Performance of Vision-and-Language Navigation Model: a Snapshot Ensemble Method”

## Appendix A: Pre-processing of Recurrent PREVALENT model

Recurrent PREVALENT does not process panoramic view  $O_i$  directly. Instead, it uses the image feature of the view  $O_{i,j}$  that leads to a particular navigable viewpoint to represent the action it goes there next. In addition, an all-zero image feature will be added to represent the stop action. In the other words, the visual inputs are the features of candidate actions:  $O_{candidate} = [O_{a_1}, \dots, O_{a_n}, O_{a_{stop}}]$ ,  $O_{candidate} \in \mathbb{R}^{(n+1) \times k_1}$ , where  $n$  is the number of navigable viewpoints to go next and  $k_1$  is the size of image feature.

On the other hand, Recurrent PREVALENT preprocesses the instruction inputs with pre-trained BERT embedding. Thus,  $I = [w_{cls}, w_1, \dots, w_L, w_{sep}]$ ,  $I \in \mathbb{R}^{(L+2) \times k_2}$  where  $L$  is the instruction length and  $k_2$  is the word embedding feature size. The  $cls$  token in  $I$  will be used as a hidden state for the recurrent process later.

To allow cross-attention between texts and images, Recurrent PREVALENT then projects the word and image features into a common feature space of size  $k_3$ :

$$F_{instruction} = IW_{instruction} = [f_{cls}, f_{w_1}, \dots, f_{w_L}, f_{sep}]$$

$$F_{candidate} = O_{input}W_{candidate} = [f_{a_1}, \dots, f_{a_n}, f_{a_{stop}}]$$

$W_{instruction} \in \mathbb{R}^{k_1 \times k_3}$  and  $W_{candidate} \in \mathbb{R}^{k_2 \times k_3}$  are learnable weight matrices.

On the other hand, Recurrent PREVALENT preprocesses the instruction inputs with pre-trained BERT embedding. Thus,  $I = [w_{cls}, w_1, \dots, w_L, w_{sep}]$ ,  $I \in \mathbb{R}^{(L+2) \times k_2}$  where  $L$  is the instruction length and  $k_2$  is the word embedding feature size. The  $cls$  token in  $I$  will be used as a hidden state for the recurrent process later.

To allow cross-attention between texts and images, Recurrent PREVALENT then projects the word and image features into a common feature space of size  $k_3$ :

$$F_{instruction} = IW_{instruction} = [f_{cls}, f_{w_1}, \dots, f_{w_L}, f_{sep}]$$

$$F_{candidate} = O_{input}W_{candidate} = [f_{a_1}, \dots, f_{a_n}, f_{a_{stop}}]$$

$W_{instruction} \in \mathbb{R}^{k_1 \times k_3}$  and  $W_{candidate} \in \mathbb{R}^{k_2 \times k_3}$  are learnable weight matrices.

Copyright © 2021, Association for the Advancement of Artificial Intelligence (www.aaai.org). All rights reserved.

## Appendix B: Curves of Validation Success Rate, Imitation Learning and Reinforcement Learning Losses Over Time during Training

Figure 1 shows the curve of validation success rate over time during training the original Recurrent PREVALENT model. Figure 2 and figure 3 show the imitation learning and reinforcement learning loss curves throughout the training process. The training setting is the same as described in section 5.2.

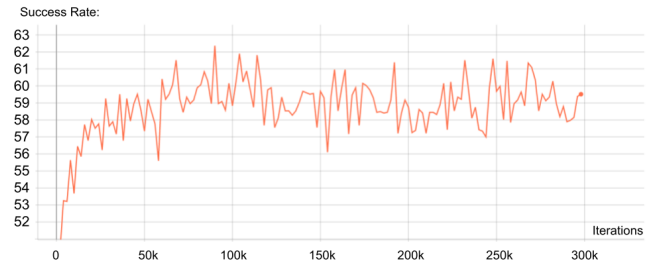


Figure 1: The curve of validation success rate over time during training. We can observe a drastic fluctuation throughout the training.

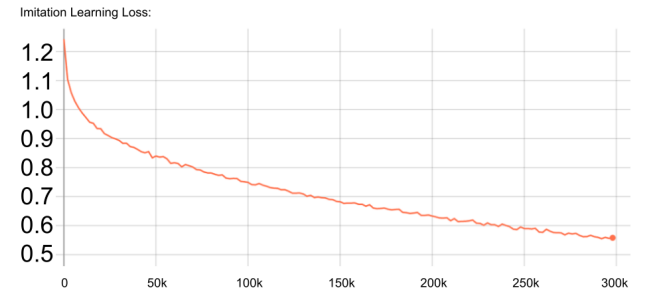


Figure 2: The curve of imitation learning loss. We can observe a consistent drop throughout the training.

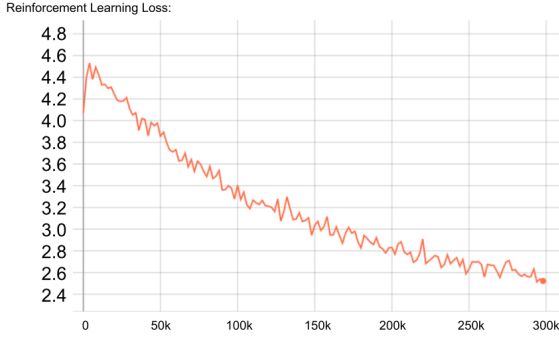


Figure 3: The curve of reinforcement learning loss. We can also see a consistent drop throughout the training.

### Appendix C: Visualization of the Attention Scores Before/After Regularization

We visualize the regularized attentions scores between  $f_{cls}^t$  and each word in the instruction feature vector  $F_{instruction}^t$ . And we also visualize the unregularized one as a comparison. The visualization is shown in figure 4. We observe that the past-action-aware modification has a more concentrated high attention word area. The red word area in the past-action-aware modification also makes more logical sense as the part of the instruction the agent focuses on.

### Appendix D: the Ablation Study for $M$ and $k$ of Snapshot Ensemble

To find out the influences of  $M$  and  $k$  on the performance of snapshot ensemble, we evaluate the performances of snapshot ensembles with different  $M$  and  $k$ 's in the R2R val.unseen split. We fixed  $k = 3$  and  $M = 10$  as the initial setting for the ablation study experiments. We tested  $M$  from  $\{5, 10, 15\}$  and  $k$  from  $\{3, 4, 5\}$ . The results are shown in table 1 and table 2.

M	TL↓	NE↓	SR↑	SPL↑
5	12	3.87	64.58	58.32
10	11.79	3.77	65.18	58.88
15	12.08	3.73	65.3	58.88

Table 1: The ablation study experiment for the number of snapshots to save  $M$ . Here we fixed  $k = 3$ . We saw significant improvement when  $M$  increases from 5 to 10 (0.40% in SR) but a minor improvement from 10 to 15 (0.12% in SR).

According to the results, we find a significant increase of SR from  $M = 5$  to  $M = 10$  (0.40%), while not that much (0.12%) from  $M = 10$  to  $M = 15$ . Considering  $M = 15$  takes 50% more ensembles to evaluate, we choose  $M = 10$  to be our number of snapshots to save during training.

After fixing  $M = 10$ , we discover that the ensemble performance improves by 0.38% when  $k$  increases from 3 to 4. A much less improvement is seen when  $k$  increases from 4 to 5 (0.13%). Since setting  $k = 5$  requires another 3,000 MB graphics card memory and extra sets of ensembles for

M	TL↓	NE↓	SR↑	SPL↑
3	11.79	3.77	65.18	58.88
4	11.8	3.75	65.56	59.2
5	11.88	3.8	65.69	59.36

Table 2: The ablation study experiment for the maximum number of snapshots to be in the ensemble  $k$ . Here we fixed  $M = 10$ . We saw an increase of SR when  $k$  increases from 3 to 4 (0.38%) but not that much from 4 to 5 (0.13%).

evaluation but with no significant improvement, we decide to choose  $k = 4$  as our number of maximum snapshots in the ensemble during beam search.

### Appendix E: Case Study for Recurrent PREVALENT Snapshot Ensemble

Figure 5 visualizes a case of our snapshot ensemble agent finishing navigation in a museum-like environment. The instruction is “Go through the large wooden doors and turn right. Pass the photos on the left and pass the second set of wooden doors. Continue going straight and stop at the chair at the end of the table.” In most time steps, we can see that all snapshots contribute to deciding what the ensemble should act next. However, exceptions exist. In time step  $t = 2$ , snapshots 1 and 3 both ignored “turn right” and voted to take action 1. As the only correct snapshot among three, snapshot 2 “forced” the ensemble to take action 2 by predicting the action with a much higher prediction score. The above observation suggests such a weighted voting mechanic helps improve the ensemble performance from its member snapshots.



#### Original:

walk out of the bathroom andstraight  
across the hall (#) walk downthe  
steps andstop (#)

#### Past-action-aware:

walk out of the bathroom andstraight  
across the hall (#) walk downthe  
steps andstop (#)



#### Original:

walk out of the bathroom andstraight  
across the hall (#) walk downthe  
steps andstop (#)

#### Past-action-aware:

walk out of the bathroom andstraight  
across the hall (#) walk downthe  
steps andstop (#)



#### Original:

walk out of the bathroom andstraight  
across the hall (#) walk downthe  
steps andstop (#)

#### Past-action-aware:

walk out of the bathroom andstraight  
across the hall (#) walk downthe  
steps andstop (#)

Figure 4: The visualization of attention scores between the  $f_{cls}^t$  and each word in the  $F_{instruction}^t$  vector from three different time steps. The greener the word is, the lower attention score it has. The more red the word is, the higher the attention score the word has. For better visualization, we replace period “.” with “( # )” in the figure. We can see a more concentrated red word area in the attention scores from the past-action-aware modification model. The red word areas from the action-aware-attention one also make more logical sense as “sub-instructions” to be focused on.

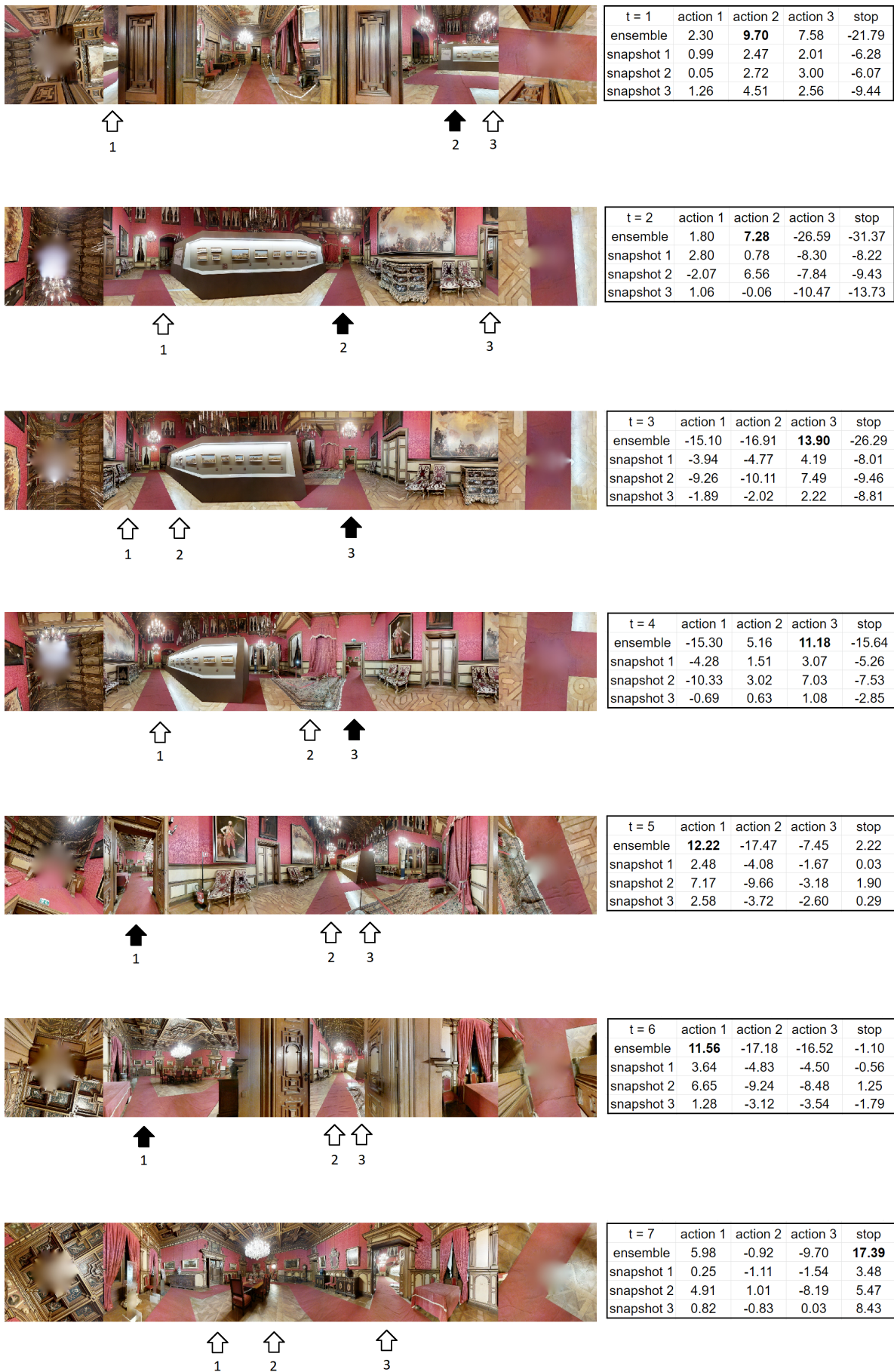


Figure 5: The visualization of the prediction scores of the ensemble and its member snapshots during navigation. The table on the right shows the prediction scores of each snapshot taking action 1, 2, 3, or stop in the current time step. The arrows below the panoramic view image point out the directions of each action goes.